UNIVERSITY OF BUCHAREST
FACULTY OF CHEMISTRY
DOCTORAL SCHOOL IN CHEMISTRY

PhD THESYS

DISCRETE AND EXTENDED POLYMETALLIC MOLECULAR SYSTEMS ASSEMBLED USING CYANOMETALLATE ANIONS AS TECTONS

ABSTRACT

PhD student:
Georgeta-Andreea Dogaru

PhD Supervisor:
Acad. Marius Andruh

2017

TABLE OF CONTENTS (*Pages and Chapters numbering is according to the PhD thesys*)

The PhD thesis „Discrete and extended polymetallic molecular systems assembled using cyanometallate anions as tectons” belongs to both fields of coordination chemistry and molecular magnetism. The work is divided into 5 chapters, comprising the state of the art (chapters I and II) and the original contributions of the candidate (chapters III, IV and V), and it concludes with a chapter of General Conclusions and anexes,

The first introductory part is divided into two sections and contains significant literature data reporting on cyano-bridge heterobi- and heterotrimetallic complexes, and their magnetic and photomagnetic properties. In the first section systems exhibiting magnetic properties such as Single Molecule Magnets (SMM), Single Chain Magnets (SCM) and spin transition are described, while the second section is devoted to the study of heterotrimetallic coordination compounds comprising three different paramagnetic metal ions. The theoretical part of the thesys justifies also the arguments that support involving polycyanometallate anions as *building-blocks* in the synthesis of new polymetallic systems:

- the ability of cyano bridge to mediate magnetic interactions;
- the high stability of these tectons towards the ligand dissociation processes;
- the existence of a large number of homoleptic $[M(CN)_x]^{n-}$ units having various compositions and geometries, such as: square antiprism or dodecahedron: $[M^{IV/V}(CN)_8]^{4-/3-}$(M = Mo, Wo), octahedral geometry - $[M^{III}(CN)_6]^{3-}$ (M = Cr, Mn, Fe, Co), square planar - $[M^{II}(CN)_4]^{2-}$ (M = Ni, Pd, Pt), tetrahedral - $[M^{II}(CN)_4]^{2-}$ (M = Zn, Cd, Hg), or linear - $[M^{I}(CN)_2]^{-}$ (M = Ag, Au).

The original contributions are presented in chapters III, IV, and V. The main research stream is represented by the synthesis and structural characterization of new polymetallic systems, using as precursors cyano-based metallo-ligands. Specifically, the directions of study are being represented by:

- synthesis of new 3d-5d-4f heterotrispin coordination compounds by employing the $[Os(CN)_6]^{3-}$ metallo-ligand as a third-spin carrier. The Os^{III} cyano-complex has been chosen not only because of the ability of the cyano bridge to mediate strong magnetic interactions, but also due to the more diffuse character of the magnetic orbitals and the aditional magnetic anisotropy (derived from the spin-orbit coupling) of the Os^{III} metal ion. The bimetallic nodes are represented by 3d-4f complexes belonging to $[CuLn(ValXn)]^{3+}$ family.

- synthesis of heterbimetallic systems by assembling polycyanometallate metallo-ligands, such as $[Mo(CN)_8]^{4-}$, $[M^{III}(CN)_6]^{3-}$ (M^{III} = Cr, Fe, Ru, Os), $[Ag(CN)_2]^{-}$, [*trans*-$Re(CN)_2Cl_4]^{2-}$ and cationic units $[M^{II}(L)]^{2+}$ (M^{II} = Co, Ni, Cu, Zn) having the metal ion coordinated by a

polydentate ligand resulted from the condensation reaction between 2,6-diacetylpyridine and 2,2-dimethyl-1,3-propanediamine.

Presentation of original contribution starts with chapter III, comprising the description of various 3d-5d-4f heterotrispin systems, assembled using anionic tectons containing Os^{III} and Os^{II} metal ions, $[Os(CN)_6]^{3-/4-}$. This chapter is divided into two sections, according to the dimensionality of the resulted system. Therefore, the first section contains discrete 3d-5d-4f compounds, while the second section comprises the description of extended mono- and bidimensional heterotrimetallic systems. The assembling cationic units are bi- and trimetallic coordination compounds of 3d and 4f ions coordinated by the Schiff base ligand, H_2L^{16}, product of condensation reaction between ortho-vanilin and 2,2-dimethyl-propylenediamine (figure 1).[1] The selection of the side-off bicompartmental ligand was justified by its ability to coordinate, simultaneously, 3d and 4f metal ions, within the two different coordination sites, both by the nature of the donor atoms, as well as by the dimension of the metal ions. At the same time, the synthesis of these heterobimetallic precursors is straightforward and the final compound is obtained in high yields.[2]

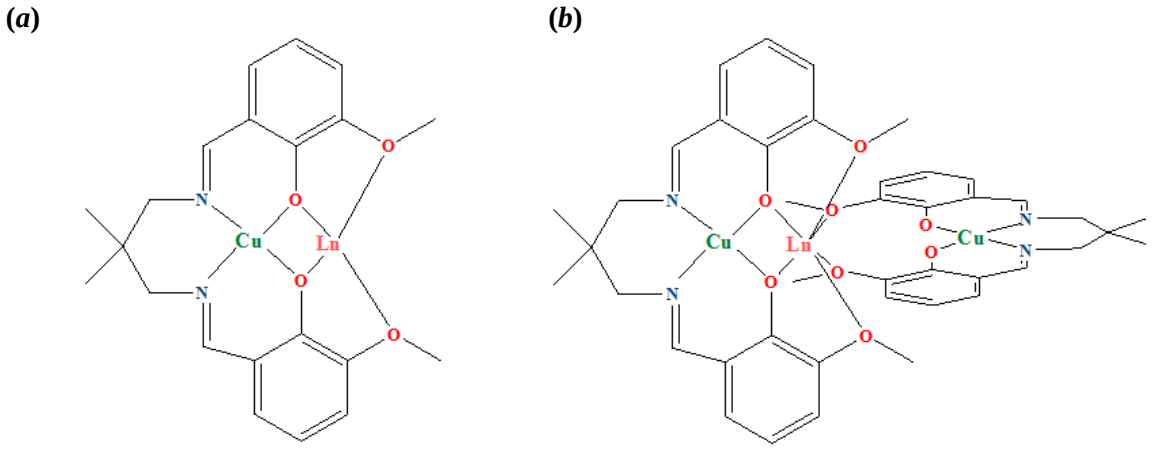

Figure 1. Oligonuclear complexes used in the synthesis of heterotrispin systems: ***(a)*** $[Cu(L^{16})Ln]$, ***(b)*** $[\{Cu(L^{16})\}_2Ln]$.

In the reaction synthesis, in addition to the bimetallic node, the $[Os(CN_6)]^{3-}$ metallo-ligand was employed, as the third spin carrier. The more diffuse character of the orbitals of the Os^{III} metal ion, within the $[Os(CN)_6]^{3-}$ species, in comparison to the Ru^{III} and Fe^{III} orbitals, respectively, as well as the aditional anisotropy (derived from the spin-orbit coupling), were the arguments that justified the employment of this precursor. The cyano-complex was synthesized in a two step reaction.[3] In the first step the Os^{II} cyano-complex was synthesized, starting from osmium tetroxide, OsO_4. Subsequently, the Os^{II} metal ion is oxidized to Os^{III}, using $Ce^{IV}(SO_4)_2$

as an oxidation agent, and the K^+ cations are replaced by $(PPh_4)^+$ cations, thus leading to the $(PPh_4)_3[Os(CN)_6]$ precursor.

The first section of this chapter contains the description of four izostructural compounds $[\{(Cu(L^{16}))_4Ln_2(H_2O)_2\}\{Os(CN)_6\}_2]\cdot 3CH_3OH\cdot 4H_2O\cdot CH_3CN$ (Ln = Sm (**1**), Gd **(2)**, Tb (**3**), Dy (**4**)), resulted from the self-assembly process between the $[\{Cu(L^{16})(H_2O)\}_2Ln(NO_3)_3]$ and $(PPh_4)_3[Os(CN)_6]$ species, in methanol:acetonitrile mixture. The heterotrinuclear compound $[\{Cu(L^{16})(H_2O)\}_2Ln(NO_3)_3]$ was obtained *in situ* in the reaction between the Cu^{II} complex, $[Cu(L^{16})(H_2O)]$, and Ln^{III} nitrates, $Ln(NO_3)_3\cdot xH_2O$. Single crystal X-ray diffraction measurements revealed the existence of an octanuclear cluster, composed of two $\{Cu_2Ln\}$ modules connected by $[Os(CN)_6]^{3-}$ metallo-ligands. The crystal structure of the heterotrinuclear compound - **2** is depicted in figure 2.

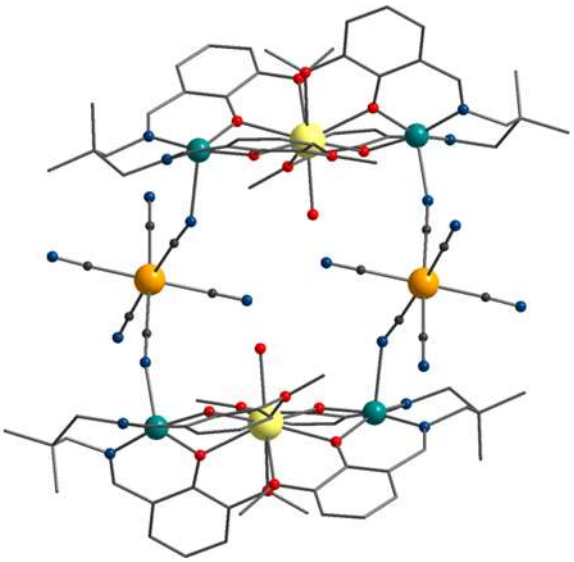

Figure 2. Molecular structure of the octanuclear compound **2**.

Within the trinuclear fragment, the Cu^{II} is hosted by the $[N_2O_2]$ compartment of the ligand, two $[Cu(L^{16})]$ units encapsulating through their outer $O_2O'_2$ compartment the Gd^{III} ion (two oxygen atoms arise from the phenoxido groups and the two others from the methoxy ones). The intra-module Cu···Gd distances are 3.522 and 3.527 Å and the diedral angle, formed by the planes defined by the donor atoms belonging to the ligand, has a value of 47.1°. The metallo-ligand, $[Os(CN)_6]^{3-}$ connects two trinuclear fragments, involving two *cis* cyano groups as bridges. The distances between the copper and osmium atoms across the cyanido bridges are: Cu1···Os1 = 5.365(14) and Cu2···Os1^i = 5.186(17) Å (^{i} = 2-x, 1-y, 2-z).

The magnetic properties of Gd^{III} and Tb^{III} systems (compounds **2** and **3**) are described in chapter III.1.3. Magnetic properties of both compounds are presented under the form of $\chi_M T$ agains *T* plots and *M* agains *H* plots, respectively, as shown in figure 3 (for compound **2**). At 270

K, the product $\chi_M T$ is equal 20.3 $cm^3mol^{-1}K$, a value compatible with the calculated value for two S =7/2 and six S = ½ non-interacting spins. By lowering the temperature, $\chi_M T$ product increases and reaches a maximum of 26.6 $cm^3mol^{-1}K$ at 8 K, indicating the occurence of ferromagnetic interactions. Below this temperature, a marked decrease of the $\chi_M T$ value is observed down to 11.2 and 8.8 cm^3mol^{-1} K at 1.85 K. The magnetization vs. field curve below 3 K show a clear saturation at high DC fields close to the expected 20 μ_B at 1.85 K.

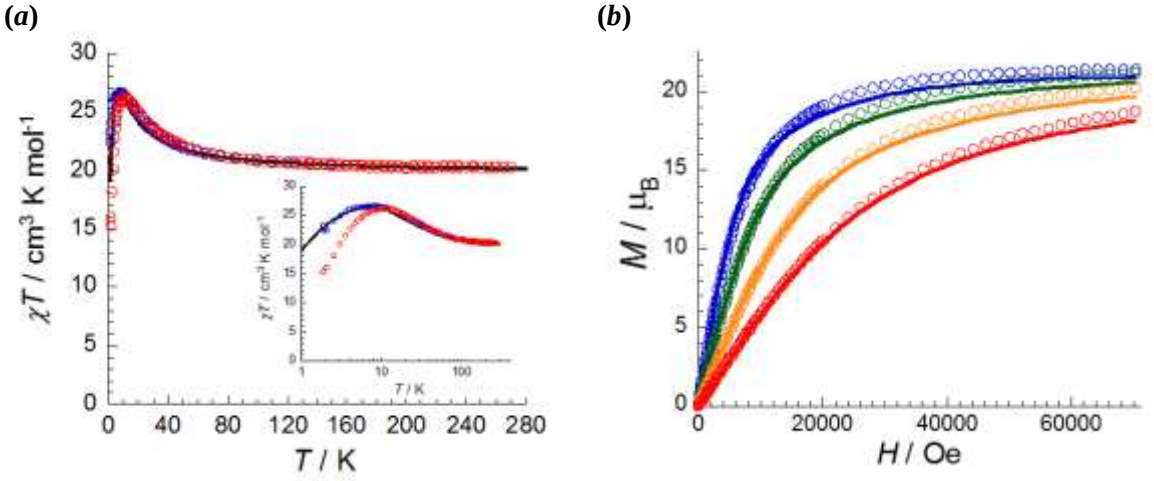

Figura 3 (*a*) Temperature dependence of the χT product (*inset*: the $\chi_M T$ *vs* T plot at 2 K); **(*b*)** Field dependence of the magnetization below 8 K for **2**.

Fitting the magnetic susceptibility data lead to the following set of parameters: $J_{Cu\text{-}Gd}$ = 2.10 cm^{-1}, $J_{Cu\text{-}Os}$ = -0.42 cm^{-1} and g_{Os} = 1.85, g_{Gd} = 2.09 g_{Cu} = 2.30.

The magnetic properties of compound **3** are similar to the ones observed for compound **2**, also showing predominat ferromagnetic interactions between Cu^{II} and Tb^{III} ions via the phenoxo bridge (figure 4).

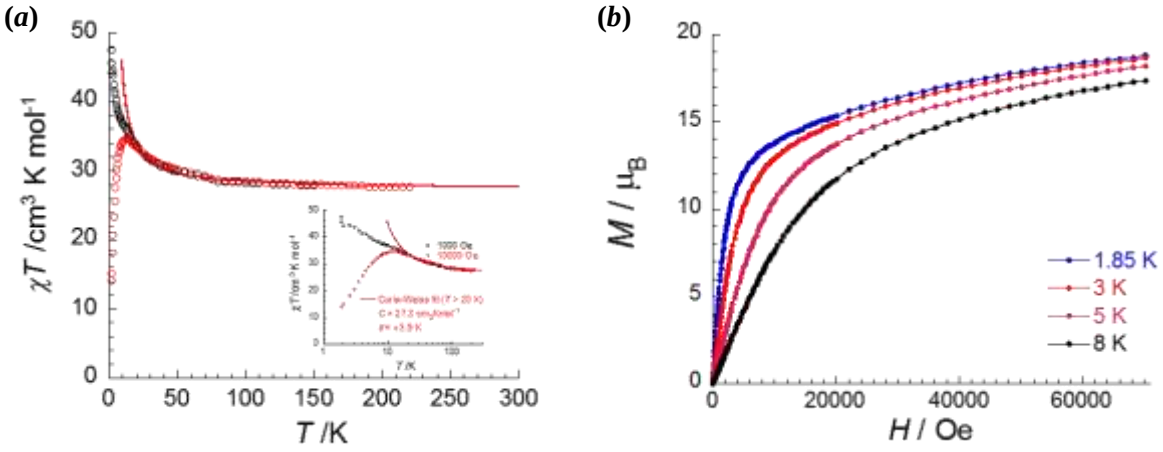

Figura 4 (*a*) Temperature dependence of the χT product (*inset*: the $\chi_M T$ *vs* T plot below 100 K); **(*b*)** Field dependence of the magnetization below 8 K for **2**.

At 270 K, the value of the $\chi_M T$ product is equal to 27.8 $cm^3mol^{-1}K$. By lowering the temperature $\chi_M T$ product increases and reaches a maximum of 45.6 $cm^3mol^{-1}K$ at 1.9 K, as a sign of the dominating Cu···Tb ferromagnetic interactions. Below this temperature, a marked decrease of the $\chi_M T$ value is observed.

In order to probe the posibility of displaying a slow dynamic of the magnetization, AC susceptibility measurements above 1.8 K, between 0 and 1 T dc field were performed for compound **3**. These measurements showed no significant frequency dependence of the imaginary components of the magnetic susceptibility (χ_M' and χ_M'', respectively).

The second section of chapter III contains the structural and spectral description of extended 3d-5d-4f systems, assembled starting from heterobi- and heterotrinuclear complexes, such as {CuLn}, and {Cu_2Ln}, respectively, and the anionic species: $[Os(CN)_6]^{3-}$. Therefore, by reacting the $(PPh_4)_3[Os(CN)_6]$ precursor with the heterobinuclear complex $[Cu(L^{16})Ln(NO_3)_3]$ (in 1:1 stoechiometry) extended mono- and bidimensional heterotrimetallic complexes were obtained: $[\{Cu(L^{16})(H_2O)Gd(H_2O)_4\}_4\{Os(CN)_6\}_3]$ (**5**), $[\{Cu(L^{16})Gd(CH_3COO)\}\{Os(CN)_6\}]$ (**6**). The presence of water solvent in the media lead to the reduction of the Os^{III} center, thus forming the diamagnetic species, $[Os^{II}(CN)_6]^{4-}$.

By comparing the two systems, one can notice a common feature: in both cases the side-off compartmental ligand accomodates the Cu^{II} and Gd^{III} ions through the different coordination sites. Therefore, the Cu^{II} ions are located in the internal compartment of the organic ligand, $[N_2O_2]$, and the Gd^{III} ions are located in the external compartment, $[O_2O_2]$, the two centers being connected through the phenoxo bridge. The coordination mode of the $[Os(CN)_6]^{4-}$ metallo-ligand lead to two different topologies. In the crystal structure of compound **5**, depicted in figure 5, one $[Os^{II}(CN)_6]^{4-}$ unit connects two Cu^{II} metallic centers, involving two *trans* cyano ligands in the coordination, while a different $[Os^{II}(CN)_6]^{4-}$ unit connects four Gd^{III} centers, involving four cyano groups as bridges, resulting a ribbon topology.

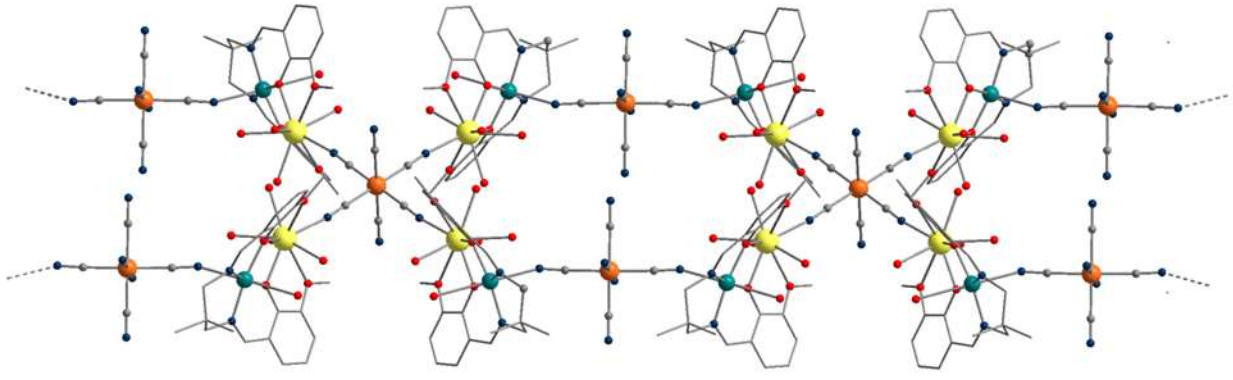

Figure 5. Crystal structure of **5**.

The crystallographic measurement perfomed for compound **6** have pointed out that the anionic unit $[Os^{II}(CN)_6]^{4-}$ connects four bimetallic fragments, involving four *trans* cyano groups in bridging two Cu^{II} centers and two Gd^{III} centers belonging to different subunits. This coordination mode, exhibited by the hexacyanometallate unit, generates a bidimensional coordination polymer, characterized by a grid-like topology (figure 6).

(*a*) **(*b*)**

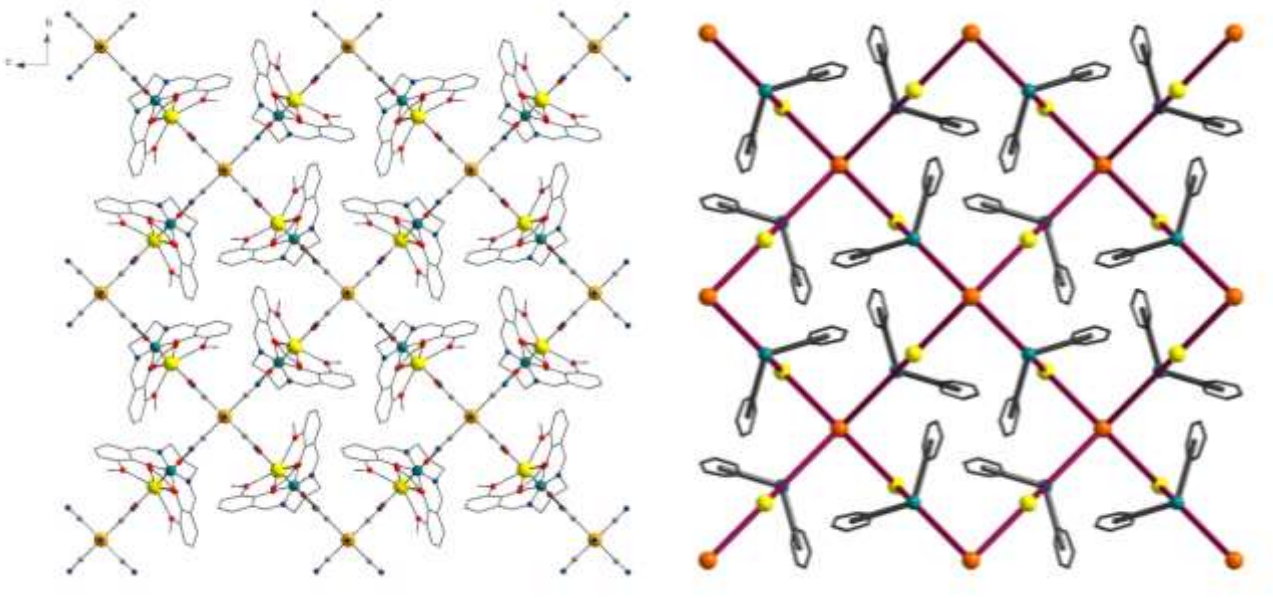

Figure 6. (*a*) Crystal structure of **6**, **(*b*)** schematic reprezentation of the grid-like topology.

In order to prevent the reduction process of the Os^{III} species, the reagents and the stoechiometries were modified. Therefore, the investigations have been oriented towards generating the trimetallic complex $[\{Cu(L^{16})(H_2O)\}_2\ Ln(NO_3)_3]$ *in situ* and reacting it with $(PPh_4)_3[Os(CN)_6]$ in methanol. This synthetic strategy lead to four izostructural systems, having the general formula $^1{}_\infty[\{(Cu(L^{16}))_2Ln(CH_3OH)\}\{Os(CN)_6\}]\cdot 5CH_3OH\cdot H_2O$, (Ln = Sm (**7**), Gd (**8**), Tb (**9**), Dy (**10**)).

Single crystal X-ray diffraction measurements revealed the existence of a one dimensional structure, a zig-zag chain. Within the structure, the $[Os(CN)_6]^{3-}$ spacers interact solely with the Cu^{II} atoms belonging to the heterotrinuclear nodes, involving two *cis* cyano groups as bridges (figure 7).

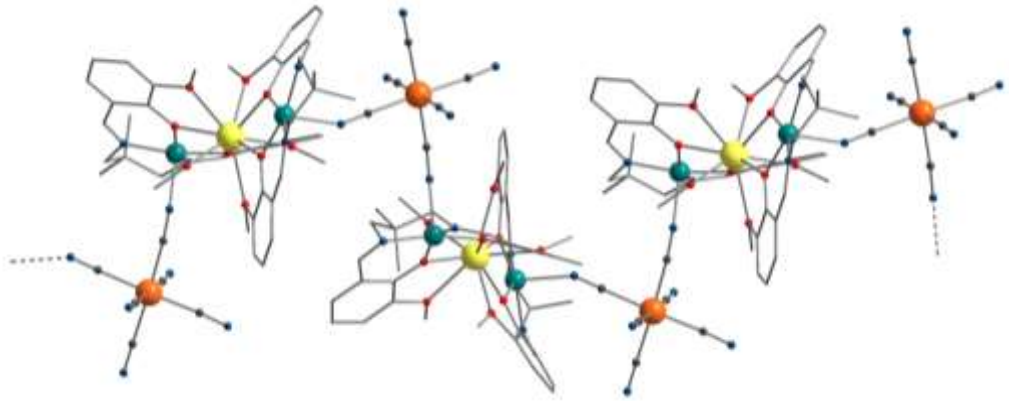

Figure 7. Crystal structure of compound **9**.

The magnetic properties for compound **8** and **9** are presented under the form of the temperature dependence of the $\chi_M T$ product (figure 8), and the field dependence of the magnetization (figure 9), respectively. By comparing the shape of the $\chi_M T$ agains T plots, recorded for octanuclear compounds (**2** and **3** presented in chapter III.1) and the ones recorded for the one dimensional compounds, **8** and **9**, one can observe a similar behaviour. By decreasing the temperature, the $\chi_M T$ value increases, indicating the occurence of ferromagnetic interactions between the Cu^{II} and Ln^{III} centers, mediated by the phenoxo bridge. Below 2 K, a marked decrease of the $\chi_M T$ value is observed, due to antiferromagnetic interactions established between the Cu^{II} and Os^{III} centers.

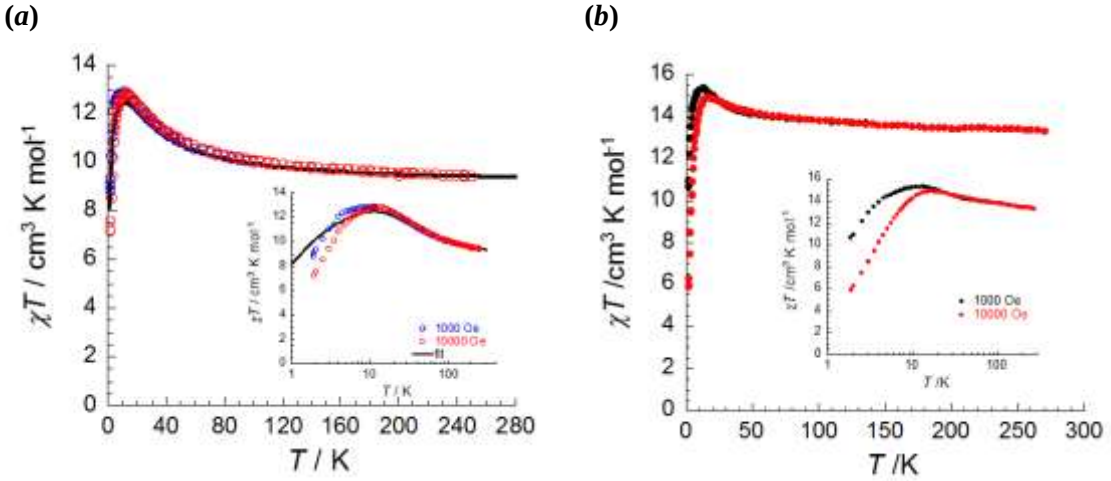

Figure 8. Temperature dependence of the $\chi_M T$ product recorded for **(*a*)** compound **8**; **(*b*)** compound **9**. *Inset* $\chi_M T$ *vs* T plots between 2 K and 100 K.

By fitting experimental data for **8**, using an Heisenberg spin Hamiltonian, the following set of parameters have been obtained: g_{Os} = 1.85, g_{Gd} = 1.99, g_{Cu} = 2.25, $J_{Cu\text{-}Os}$ = -0.44 cm^{-1}, $J_{Cu\text{-}Gd}$ = 3.73 cm^{-1}, zJ = -0.005 cm^{-1}.

By representing the field dependence of the magnetization plot for **8** (figure 9 (*a*)) one can observe that the magnetization reaches the saturation value of 10 Nβ (the expected value for a system containing 10 electrons) below 3 K.

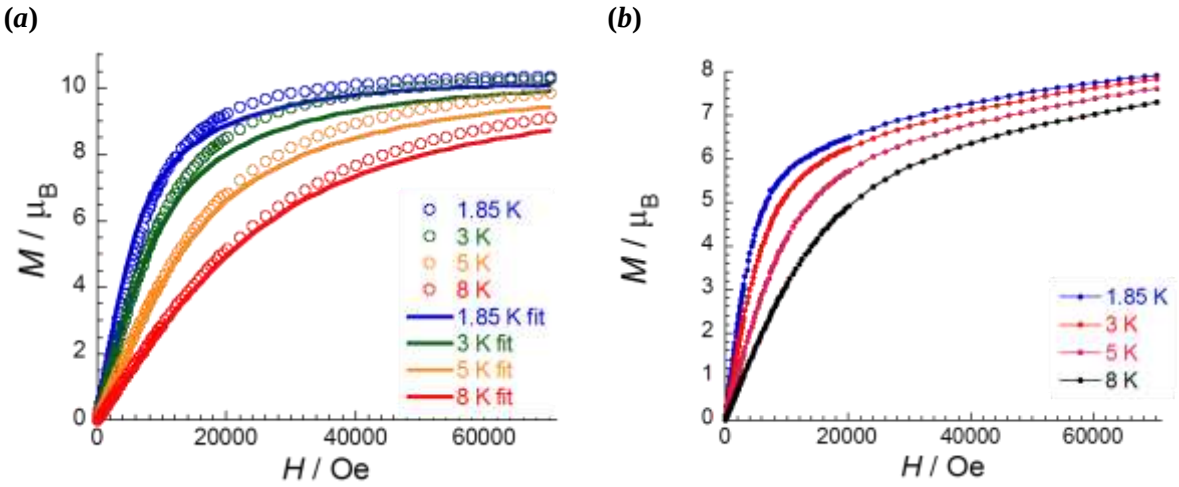

Figure 9. Field dependence of the magetisation recorded for **(*a*) 8** and **(*b*) 9**.

In the AC measurements, the frequency dependence of the imaginary component of magnetic susceptibility χ_M" *(out-of-phase*, absorbtive), recorded for **9**, is insignificant.

The magnetic behaviour of **2**, **3**, **8** and **9** can be understood taking into account that the:

- the Cu^{II}-Gd^{III}/Tb^{III} interaction within bi- and trinuclear complexes with ValXn ligands is in most cases ferromagnetic;

- the M^{III} (d^5, *low-spin*) -CN-Cu^{II} interaction is generally weak, since it involves the apical positions of the Cu^{II} center, the magnetic orbital ($d_{x^2-y^2}$) being located in the bazal plane.

The second research direction within the PhD thesys is represented by the synthesis of new cyano-bridge heterobimetallic complexes using as assembling units:

- cationic complexes of Ni^{II}, Cu^{II} and Zn^{II} with Schiff-base ligands, derived from 2,6-diacetylpyridine.

- homoleptic and heteroleptic cyano complexes, such as $[M(CN)_x]^{n-}$ (M = Mo^{IV}, Cr^{III}, Fe^{III}, Ru^{III}, Os^{III}, Ag^{I}), and $[Re^{IV}(CN)_2Cl_2]$. Cyanometallate precursors containing Mo^{IV}, Ru^{III}, Os^{III} and Re^{IV} were prepared according to the literature.[3]

By assembling these units heterobimetallic complexes of different dimensionalities (2-D, 1-D, 0-D) were obtained and described in chapters IV and V.

Chapter IV contains the comparative analysis of two bidimensional systems synthesized using hexacyanometallate anions of Fe^{III} and Co^{III} as metallo-ligands. The assembling cations are represented by complexes of Fe^{III} and Co^{III} with a pentadentate macrocyclic ligand, obtained by

the template condensation reaction between 2,6-diacetylpyridine and 3,4-dioxaoctane-1,8-diamine, and triethylenetetramine, respectively (figure 10).

The macrocyclic ligands usually coordinate into the equatorial plane of the metal ion, the axial position being accessible to auxiliary ligands, such as cyano or oxalate groups. Moreover, they favour a pentagonal bipyramidal geometry around metal ions, can enhance the local magnetic anisotropy and their coordination prevents the oxidation of M^{II} to M^{III} metal ions.

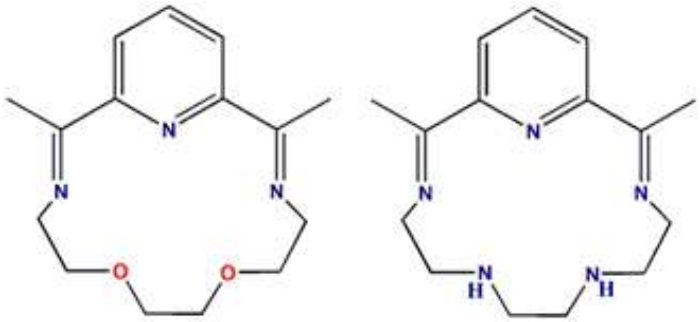

Figure 10. Macrocyclic pentadentate ligands.

The bidimensional complex $[\{Co(L^{19})\}_3\{Fe(CN)_6\}_2]\cdot 6CH_3OH\cdot 6H_2O$ - **11** was obtained as a single crystal through slow diffusion in test tubes and has been structurally and spectroscopically characterized. The asymmetric unit for **11**, presented in figure 11, reveals two crystallographically independent heptacoordinated cobalt ions, both with a pentagonal bipyramidal stereochemistry. Their equatorial plane is formed by two oxygen atoms and three nitrogen atoms, belonging to the organic ligand, while the apical positions are being occupied by nitrogen atoms arising from the cyano bridges.

The $[Fe(CN)_6]^{3-}$ building-block involves three facial cyano ligands as bridges. Each hexacyanoferrate anion is connected to three cobalt ions and each cobalt center is connected to two anionic $[Fe(CN)_6]^{3-}$ units, resulting into a distorded honeycomb topology.

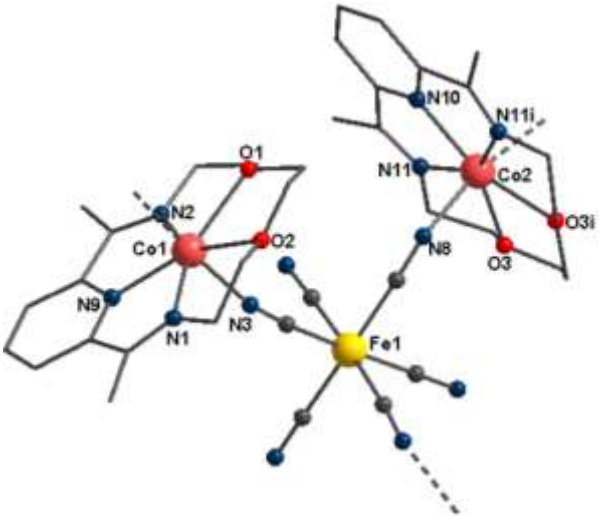

Figure 11. The asymmetric unit of compound **11**.

Using as assembling units the Fe^{II} complex, $[Fe(L^{20})(H_2O)_2]Cl_2$, and the Co^{III} hexacyanometallate precursors, $[Co(CN)_6]^{3-}$, in similar conditions, Clérac *et al*. reported on the bidimensional $[\{Fe(L^{20})\}_3\{Co(CN)_6\}_2]\cdot 2CH_3OH\cdot 13H_2O$ compound.[4] Within its structure, each $[Co(CN)_6]^{3-}$ unit involves three meridial cyano groups as bridges, resulting into a distorted brick wall topology. The crystal structures of both bidimensional compounds $[\{Co(L^{19})\}_3\{Fe(CN)_6\}_2]\cdot 6CH_3OH\cdot 6H_2O$ (**11**) and $[\{Fe(L^{20})\}_3\{Co(CN)_6\}_2]\cdot 2CH_3OH\cdot 13H_2O$ are depicted, for comparison, in figure 12.

(*a*) **(*b*)**

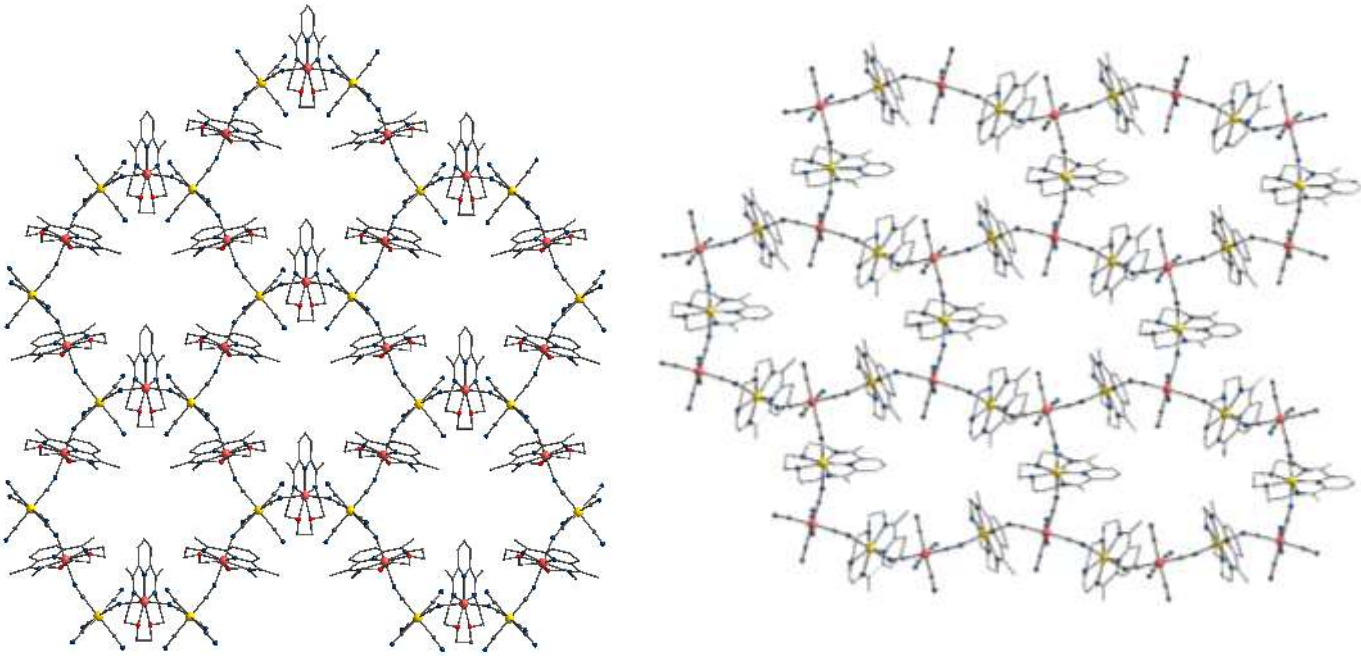

Figura 12. Crystal structures of both bidimensional systems **(*a*)** $[\{Co(L^{19})\}_3\{Fe(CN)_6\}_2]\cdot 6CH_3OH\cdot 6H_2O$ (**11**) and **(*b*)** $[\{Fe(L^{20})\}_3\{Co(CN)_6\}_2]\cdot 2CH_3OH\cdot 13H_2O$, respectively.

The different topologies are driven by the relative position of the three bridging groups from the hexacyanidometallo-ligand (facial and meridional). A schematic representation is ilustrated in figure 13.

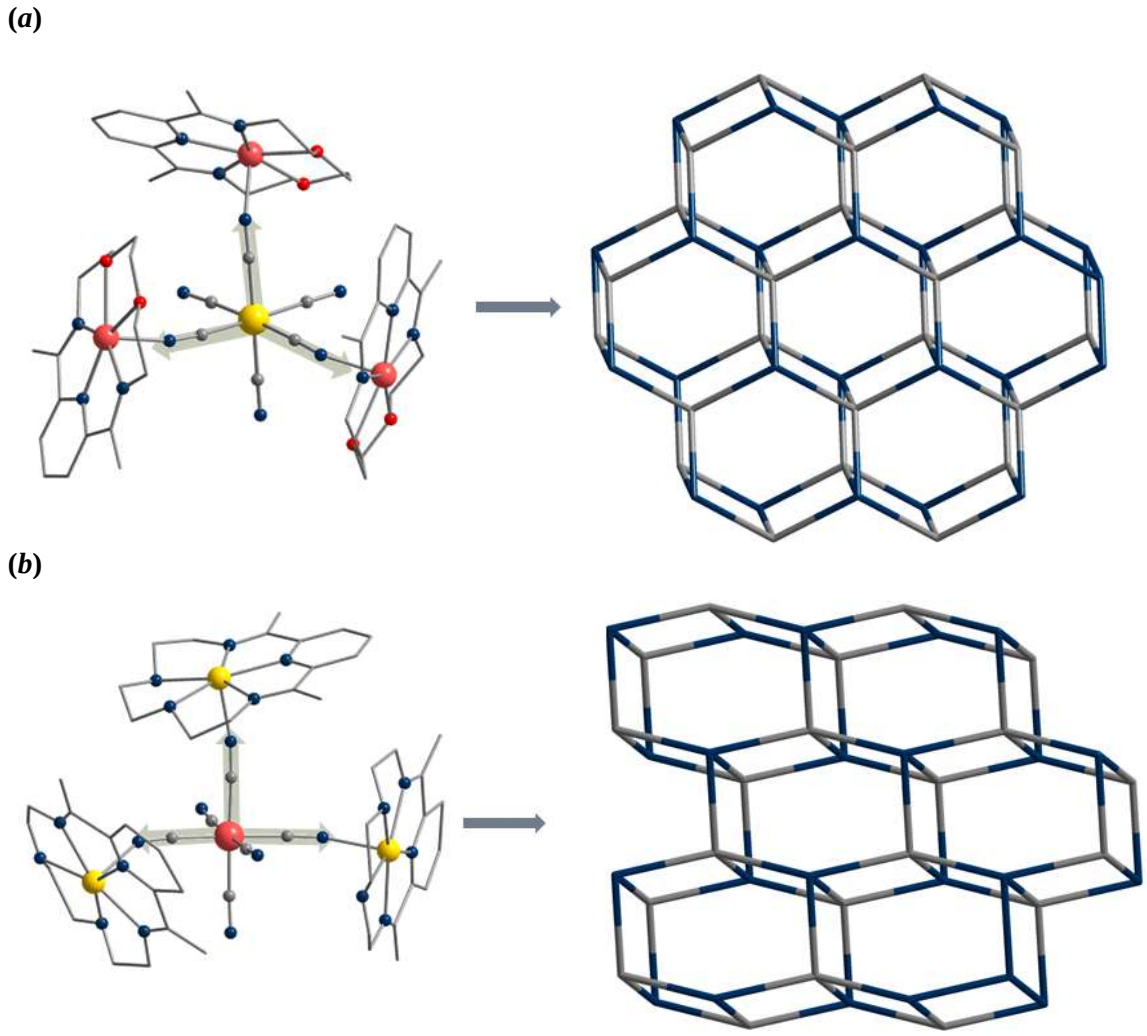

Figure 13. Schematic representetion of **(*a*)** honeycomb and **(*b*)** brick-wall topologies driven by the relative position of the three bridging groups from the hexacyanidometallo-ligand.

The magnetic properties of compound **11** were investigated. The magnetic susceptibility shown as a $\chi_M T$ versus T plot is represented in Figure 14. The room temperature value of the $\chi_M T$ product, 10.8 $cm^3mol^{-1}K$, corresponds to the value expected for three *high-spin* Co^{II} and two *low- spin* Fe^{III} non-interacting magnetic centers, having in mind that both *high-spin* Co^{II} and *low-spin* Fe^{III} ions are characterized by significant orbital contributions to their magnetic moment. By decreasing the temperature, $\chi_M T$ product increases slowly, then more abruptly, indicating dominant ferromagnetic interactions between the Co^{II} and Fe^{III} ions through the cyano bridge. Below 2.7 K, $\chi_M T$ decreases due to a saturation associated to the long-range magnetic order, also supported by the field dependence of the magnetization: below 3 K the magnetization increases very fast at low field (figure 14 (*b*)).

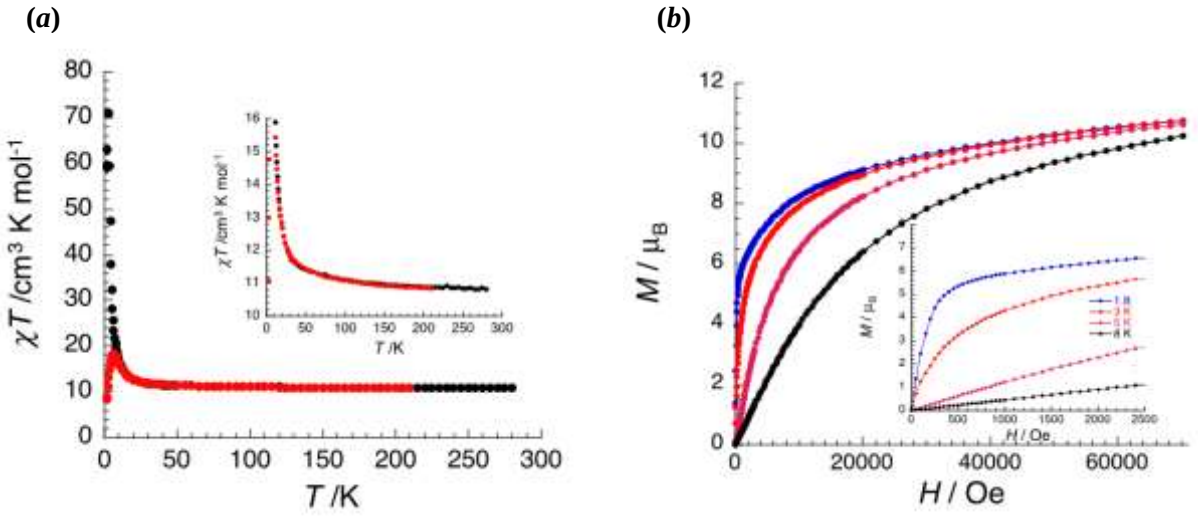

Figure 14. (*a*) Temperature dependence of the $\chi_M T$ product and **(*b*)** field dependence of the magnetization, recorded for compound **11**.

This magnetic order is further confirmed by the AC measurements displaying an out-of-phase susceptibility χ_M'' different to zero below 3 K. A small frequency dependence of the in-phase χ_M' and out-of-phase χ_M'' components is observed (figure 15).

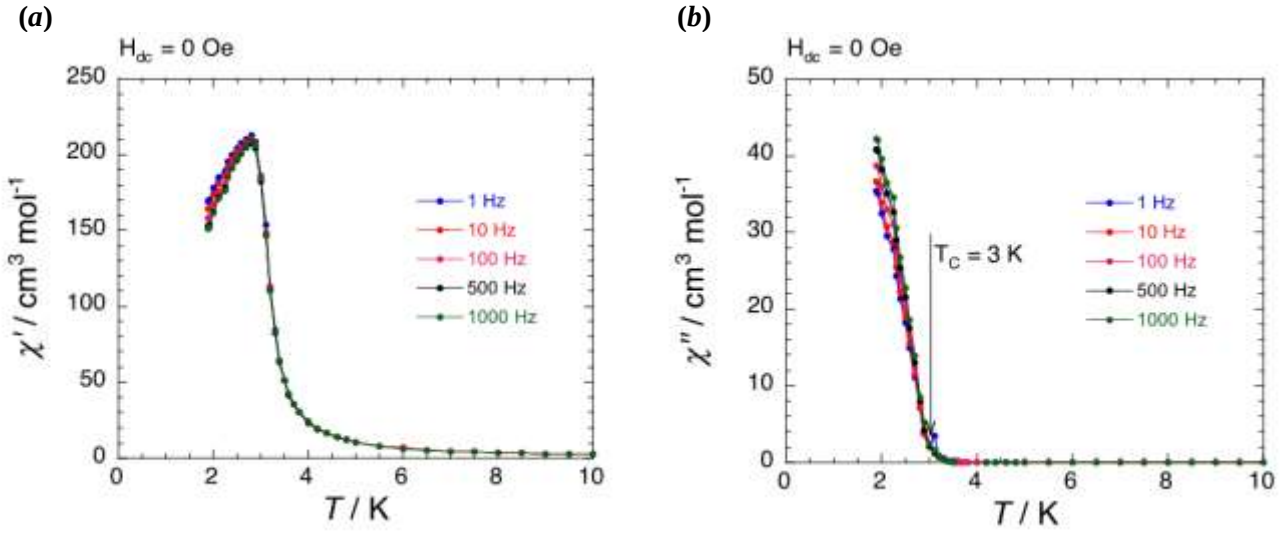

Figure 15. Temperature dependence below 10 K of the (*a*) in-phase (χ_M') and (*b*) out-of-phase (χ_M'') components of the ac susceptibility at different temperatures, recorded for compound **11**.

By using as assembling units mononuclear complexes of Ni^{II}, Cu^{II} and Zn^{II} with Schiff-base ligands, derived from the condensation reaction between 2,6-diacetylpyridine and 2,2-dimethyl-1,3-diaminopropane, low-dimensional systems are obtained. These compounds are described in chapter V.

The synthetic strategies and structural characterizations of the cationic precursors are discussed in section V.1. Mononuclear complexes, having the general formula $[M^{II}(L^{21})](ClO_4)_2$, where M^{II} = Ni (**12**), Cu (**13**) and Zn (**14**) were synthesized following similar synthetic

procedures. The compounds were obtained as brown (Ni^{II}), green (Cu^{II}) and yellow (Zn^{II}) crystals, respectively, by the template condensation reaction between 2,6-diacetylpyridine and 2,2-dimethyl-1,3-diaminopropane (1:2 stoechiometry), in the presence of M^{II} perchlorate, in methanol. The crystal structures of the precursors are depicted in figure 16. Crystallographic analysis confirms the existence of a mononuclear compound comprising a M^{II} center coordinated by 5 nitrogen atoms belonging to the Schiff-base ligand. The pozitive charge of the monocation $[M^{II}(L^{21})]^{2+}$ is compensated by two ClO_4^- anions.

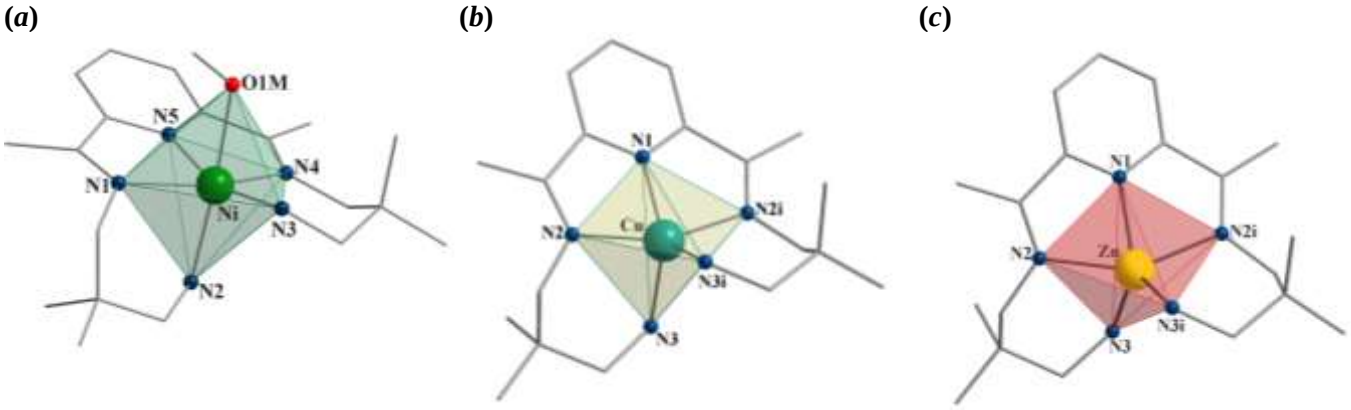

Figure 16. Crystal structures of **(*a*) 12**, **(*b*) 13** și **(*c*) 14**.

^{1}H RMN and ^{13}C RMN spectra were recorded for the mononuclear complex containing diamagnetic Zn^{II} metal ion. The ^{1}H RMN spectrum for compound **14** is depicted in represented in figure 17 and the signal interpretation is discussed in table 1.

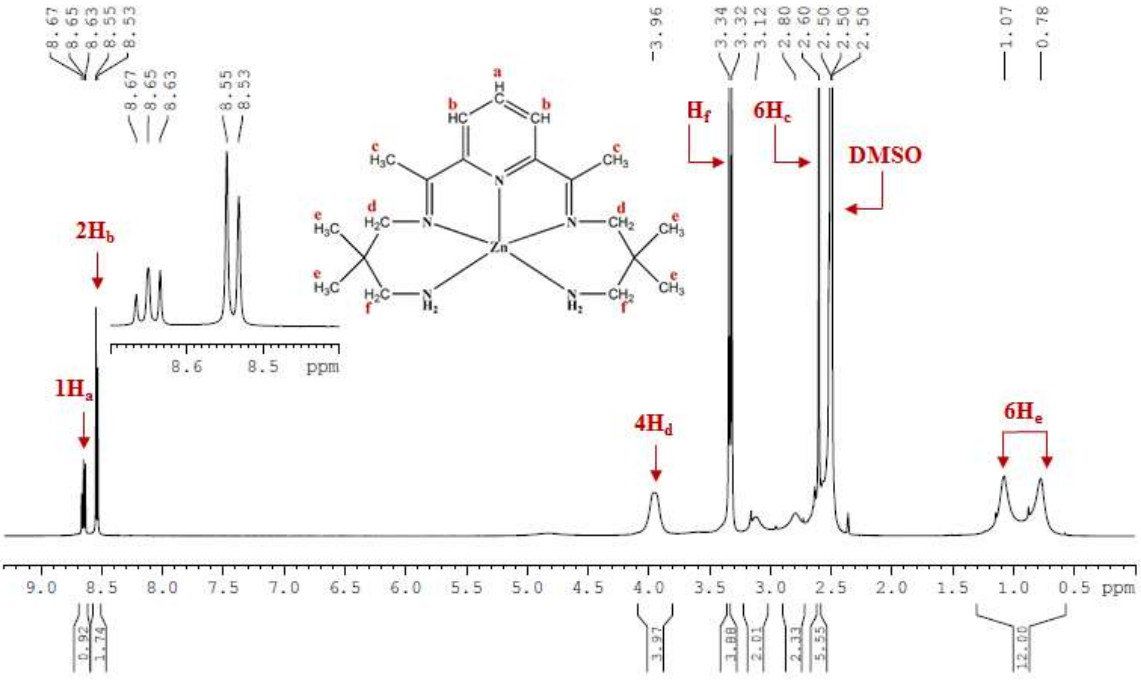

Figure 17. ^{1}H RMN spectrum recorded for compound **14**.

Table 1. ^{1}H RMN signal interpretation for compound **14**.

δ (ppm)		
8.65 (triplet)	**1 H_a proton**	**Aromatic nucleus**
8.54 (dublet)	**2 H_b protons**	
3.96 (singlet)	**4 H_d protons**	**CH_2 groups (in the proximity of imino groups)**
3.33 (dublet)	**4 H_f protons**	**CH_2 groups (in the proximity of amino groups)**
2.60 (singlet)	**6 H_c protons**	**CH_3 groups (belonging to 2,6-diacetylpyridine)**
1.07 (multiplet)	**12 H_e protons**	**CH_3 groups (belonging to 2,2-dimetyl-1,3-diaminopropane)**

Section V.2 contains the results obtained from the self-assembly process involving the mononuclear precursors, presented in section V.1, and anionic building-blocks, such as $[M(CN)_x]^{n-}$, where M = Mo^{IV}, Cr^{III}, Fe^{II}, Ru^{II}, Os^{II}, Ag^{I}.

Three new trinuclear complexes were isolated in the reaction process involving homoleptic $[M(CN)_6]^{3-}$ species (M^{III} = Fe, Ru, Os), and the complex cation $[M^{II}(L^{21})]^{2+}$. During the assembly process, a cycloaddition of one primary amine group to the -C≡N- bond is observed, resulting in a 1,3-diazacyclohexane ring (ligand L^{22}). The structures of the distinct cationic units within compounds **12** ÷ **14**, and, **15** ÷ **17**, respectively, are represented by comparison in scheme 1, being highlighted the modification of the organic ligand: L^{21} *vs.* L^{22}.

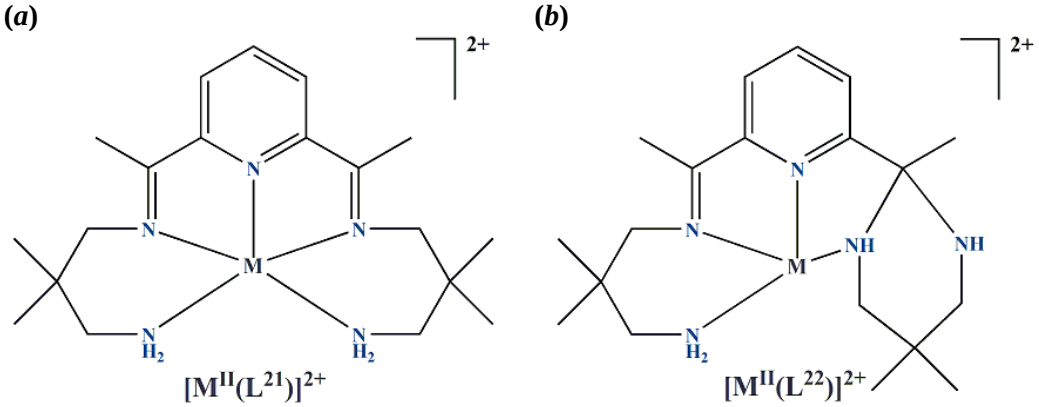

Scheme 1. Structures of cationic units within compounds **(*a*) 12** ÷ **14** and **(*b*) 15** ÷ **17**, respectively.

Using water as a solvent lead to the reduction of the paramagnetic metal ion within the $[M(CN)_6]^{3-}$ species, generating the diamagnetic precursor, $[M(CN)_6]^{4-}$.

The trinuclear complex $[\{Cu(L^{22})\}_2\{Cr^{III}(CN)_6\}]\cdot 2ClO_4\cdot 5H_2O$ - **18** was obtained by reacting the $[Cu^{II}(L^{21})]^{2+}$ complex generated *in situ* and the anionic Cr^{III} building-block, $[Cr(CN)_6]^{3-}$. A comparative analysis of the crystal structures of compounds **15** ÷ **18**, shows a common feature: the presence of the 1,3-diazacyclohexane ring generated by the addition of one amino group to the azomethinic bond. The crystal structure of the trinuclear compound, **18**, is depicted in figure 18. The non-linear structure of this compound is rationalized by the coordination mode of the $[Cr(CN)_6]^{3-}$ subunits, since it involves two *cis* cyano-groups as bridges.

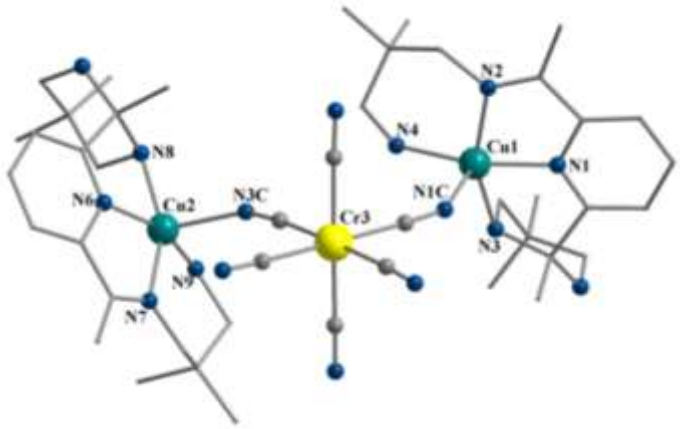

Figure 18. Crystal structure of **18**.

Crystals of compound **19** - $[\{Cu(L^{22})\}\{Ag(CN)_2\}]\{Ag(CN)_2\}$ were obtained upon the slow evaporation of a water:ethanol mixture containing the two precursors: $[Cu^{II}(L^{21})]^{2+}$, and, $K[Ag(CN)_2]$, respectively. Crystallographic data revealed the formation of a heterobinuclear cyano-bridged Cu^{II}-Ag^{I} complex, co-crystallized with an uncoordinated dicyanoargentate anion. The crystal structure of the compound is represented in figure 19.

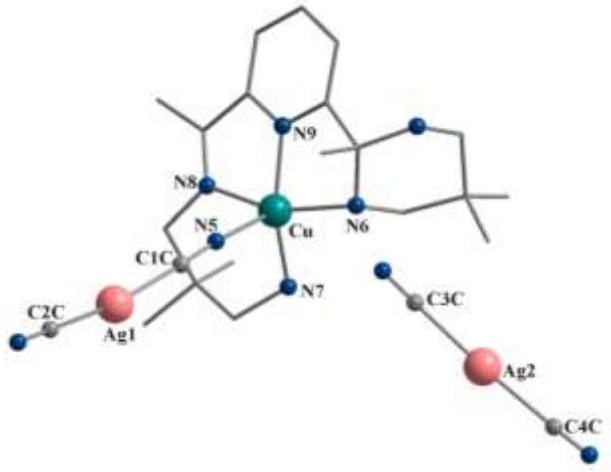

Figure 19. Crystal structure of **19**.

In order to obtain a system with a possible photomagnetic behaviour, we employed the anionic $[Mo(CN)_8]^{4-}$ units, in the assembly process, along with the cationic $[M^{II}(L^{21})]^{2+}$ (M^{II} = Cu, Zn) complexes. The results generated by this strategy consists of two trinuclear compounds $[\{Cu^{II}(L^{22})\}_2\{Mo(CN)_8\}]\cdot 18H_2O$ - **20** and $[\{Zn^{II}(L^{22})\}_2\{Mo(CN)_8\}]\cdot 2CH_3CH_2OH\cdot 7H_2O$ - **21**. The synthetic strategy is similar to the one used in the synthesis of the trinuclear complexes **15** ÷ **17**, and implies the template reaction between 2,6-diacetylpyridine and 2,2-dimethyl-1,3-diaminopropane, in the presence of M^{II} salts (1:2:1 stoechiometry), in ethanol, and the addition to this solution of an aqueous solution containing $[Mo(CN)_8]^{4-}$ species. The compounds were isolated as green (**20**) and yellow crystals (**21**), by slow evaporation at room temperature. The crystal structures of both compounds are depicted in figure 20 and 21, respectively.

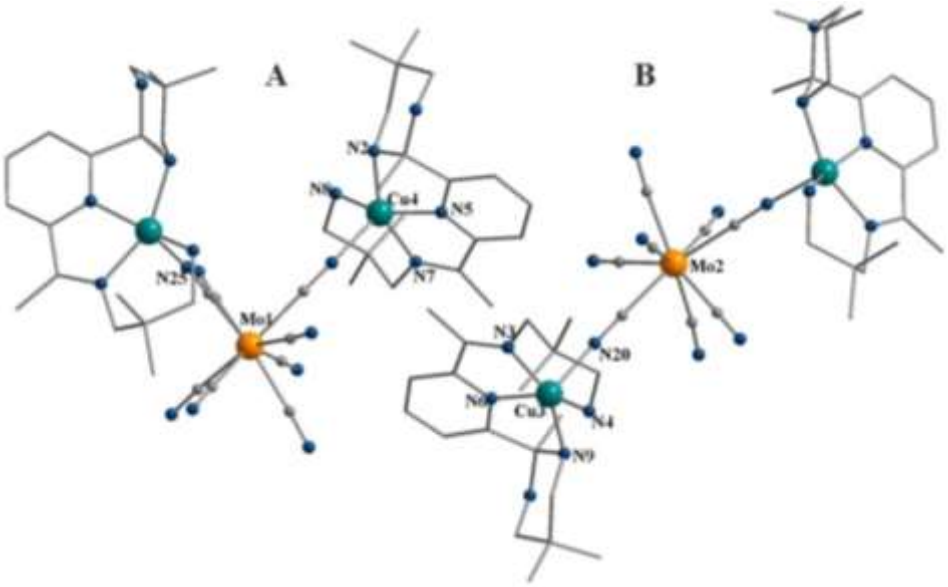

Figure 20. Crystal structure of $[\{Cu^{II}(L^{22})\}_2\{Mo(CN)_8\}]\cdot 18H_2O$ - **20**.

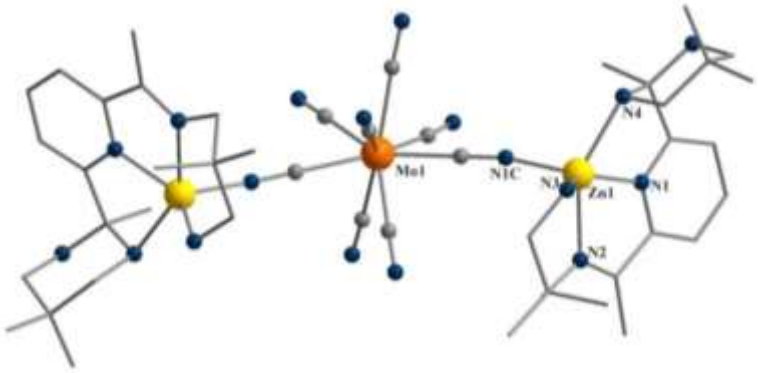

Figure 21. Crystal structure of $[\{Zn^{II}(L^{22})\}_2\{Mo(CN)_8\}]\cdot 2CH_3CH_2OH\cdot 7H_2O$ - **21**.

The structures of $\{M_2Mo\}$ compounds present the same characteristic observed within the crystal structures of the above-described systems: the Schiff-base ligand is modified as a result of the addition of two amino groups to one carbonil group.

Having in mind that these two systems contain the light-sensitive building-block, $[Mo(CN)_8]^{4-}$, in order to observe a modification of the electronic structure as a result of irradiation (photooxidation or electron transfer), reflectivity measurements were performed, by irradiating the sample using different wavelenghts, at various temperature. The thermal variation of the reflectivity spectra has been investigated, in the temperature range from 10 to 275 K. The absolute reflectivity (AR) was measured and is related to the absorption (A) with the relation AR = 1-A. The thermal dependence of the reflectivity spectra (cooling and heating modes at 4 K/min) show no effect on the optical behaviour of the compound (figure 22 (*a*) and (*b*), respectively).

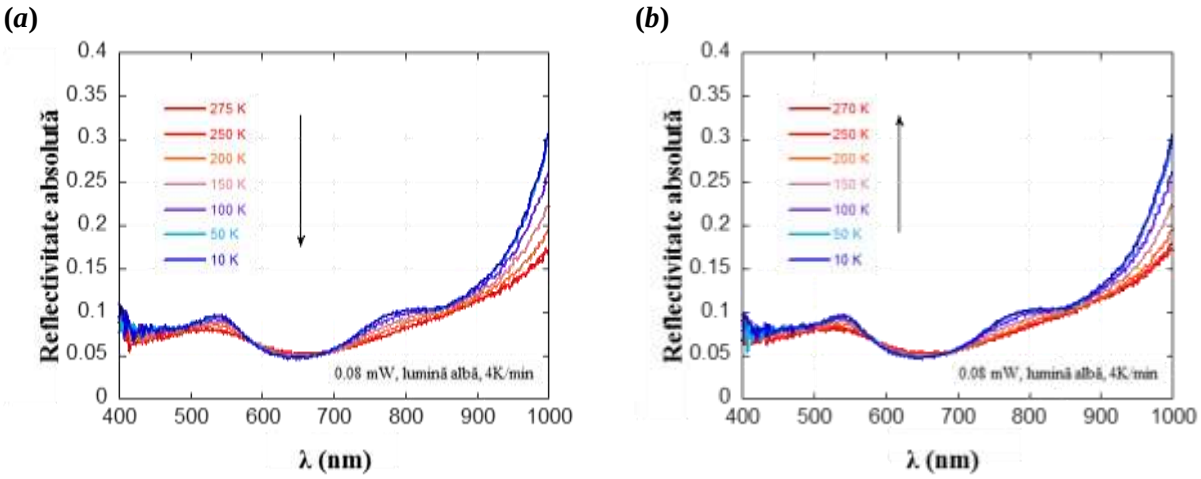

Figure 22. Temperature dependence of the reflectivity spectra of compound **20** in **(*a*)** - cooling **(*b*)** - heating mode.

Secondly, we studied the reflectivity spectra of the compound while irradiating the sample using LEDs from 1050 nm to 385 nm. By analysing the Absolute Reflectivity versus wavelenghts plots we observed no significative changes of the optical behaviour by irradiation. This observation led us to conclude this compound is not photomagnetic.

Absolute reflectivity spectra of compound **21** were carried out in a similar way as for compound **20**. Irradiating the sample using wavelenghts below 500 nm lead to observing a small modification of the optical behaviour. Having this in mind, we started a new experiment by irradiating the sample using a 385 nm LED, for 30 minutes, at low temperatures (T = 10 K), and reheating the sample (T = 274 K), in order to probe the reversibility of the process. The results of

this experiment are depicted in figure 23. One can observe a major modification of the spectra, as a result of irradiation, the modification being partially reversible by heating up to 274 K.

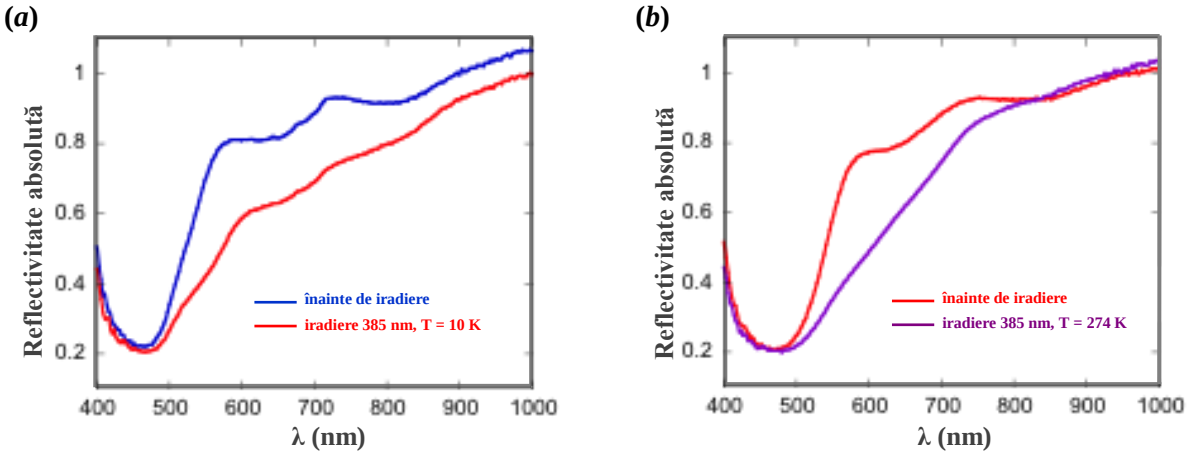

Figura 23. Reflectivity spectra of compound **21** as a result of **(*a*)** irradiation using 385 nm LED, follwed by **(*b*)** reheating the sample up to 274 K

To probe if photoreversibility can occur in this compound, we irradiated the compound at 10 K with the following sequence: excitation at 405 nm at 2 mW for 25 min and de-excitation at 625 nm for 30 min at 2 mW. The results of this study, ilustrated in figure 24, show a partial photo-reversibility of the optical behaviour.

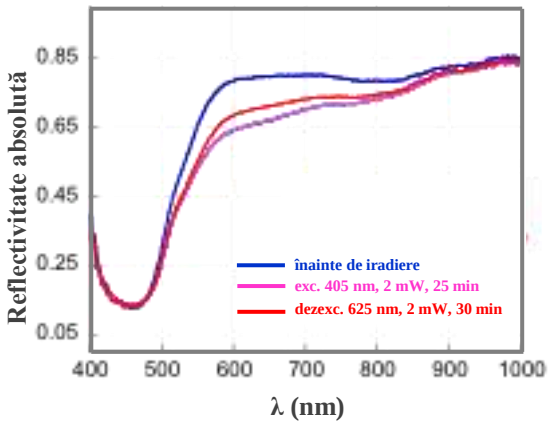

Figure 24. Reflectivity spectra of compound **21**, as a result of irradiation using 405 and 625 nm LEDs.

The graphical representation of the $\chi_M T$ product versus temperature (figure 25), that serves to highlight the magnetic behaviour of compound **20**, shows an extremely weak coupling between de Cu^{II} ions, mediated by [NC-Mo(CN)$_6$-CN] links that bridge the paramagnetic centers.

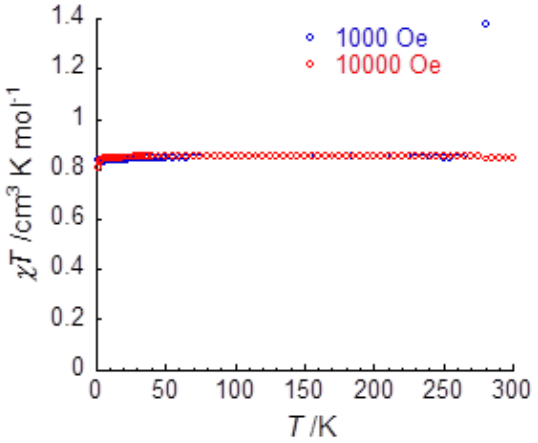

Figure 25. $\chi_M T$ versus T representation for compound **20**.

Modifying the organic ligand, using 2-aminoethyl-pyridine in the template reaction along with 2,6-diacetylpyridine, in the presence of $Ni(ClO_4)_4 \cdot 6H_2O$, and assembling the complex with the $K_4[Mo(CN)_8]$ building-block, lead to a pentanuclear cluster, $[\{Ni(L^{23})_4\}\{Mo(CN)_8\}] \cdot 4(ClO_4) \cdot 8H_2O$ - compound **23**. Within the structure four $[Ni(L^{23})]^{2+}$ cationic units are connected by one $[Mo(CN)_8]^{4-}$ anionic species, through four cyano groups. The crystal structure of **23** is ilustrated in figure 26.

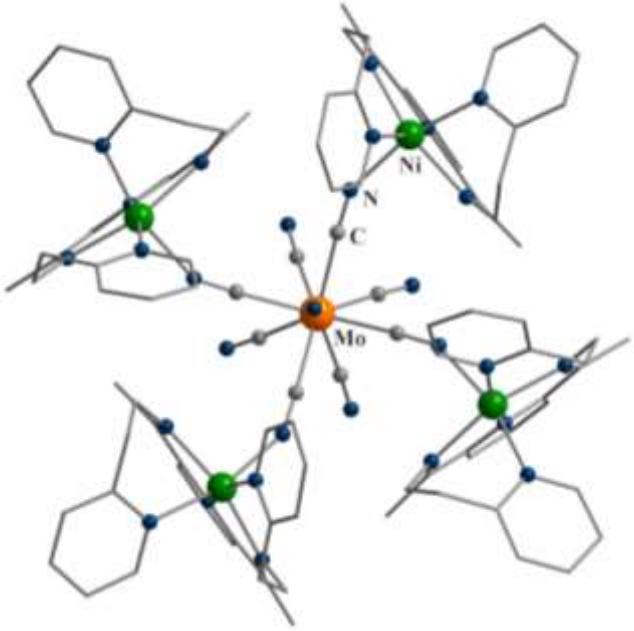

Figure 26. Crystal structure of $[\{Ni(L^{23})_4\}\{Mo(CN)_8\}] \cdot 4(ClO_4) \cdot 8H_2O$ **- 23**.

Apart from discrete heterobimetallic cyano-bridged systems, compounds **15** ÷ **23**, one coordination polymer is presented in chapter V: $[\{Cu(L^{24})_2\}\{Cu(L^{24})\}\{Mo(CN)_8\}_n] \cdot 10H_2O$, compound **24**. This compound was synthesized by reacting Cu^{II} perchlorate, N,N-dimethyl-

ethylenediamine and $K_4[Mo(CN_8)]$ in water:ethanol mixture. The chain structure of compound **24** is ilustrated in figure 27.

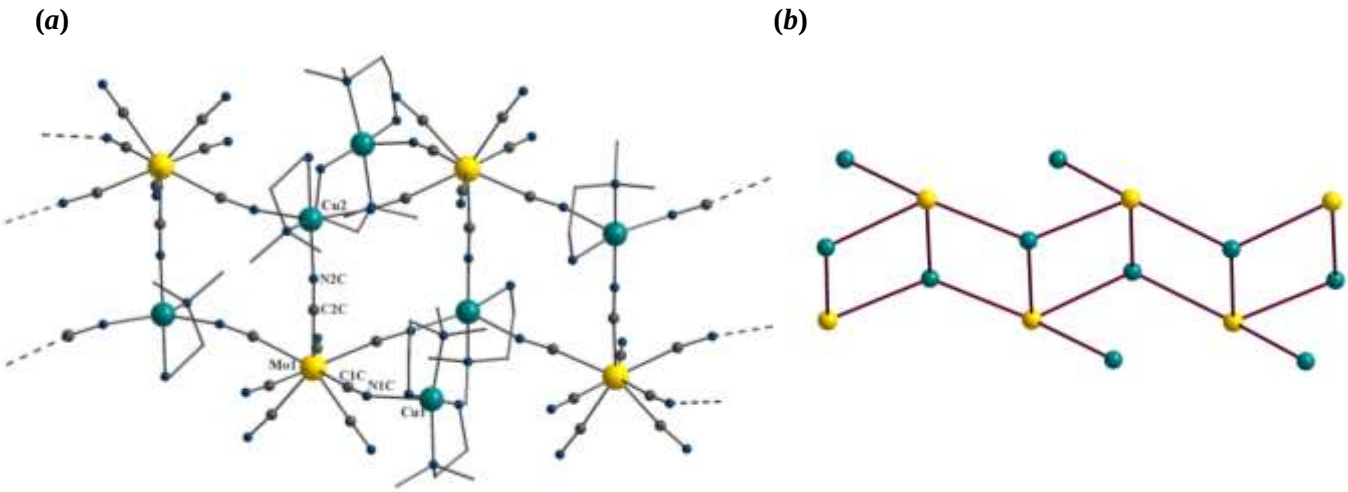

Figura 27. (*a*) Crystal structurea and **(*b*)** schematic reprezentation of the chain-like structure of compound **24**.

The reflectivity measurements, performed for this compound, showed no photo-induced effect, therefore this system is not photomagnetic

In most cases, the dimensionality of the solid state network is increased, by means of non-covalent π-π interactions (established between the aromatic fragments provided by the organic ligands), or by hydrogen bonding (involving both crystallization solvent molecules, as well as terminal cyano groups).

The research carried out in this paper accomplished its aim by synthesizing and characterizing 23 new compounds with different dimensionalities and nuclearities. Spectroscopic properties (IR and UV-vis, respectively) were investigated for all the compounds, and magnetic measurements were carried out for the heterotrispin systems **2**, **3**, **8** and **9** and for the heterobimetallic systems **11**, **20** and **24**. A particular attention was given to compounds comprising the anionic tecton $[Mo(CN)_8]^{4-}$, **20**, **21** and **24**, by studying the optical behaviour of these systems, under irradiation with different LEDs.

The PhD thesys concludes with the General Conclusions chapter and the anexes, comprising synthetic protocols, FTIR and UV-vis spectra recorded for all the compounds, the reflectivity studies, the experimental techniques, crystallografic data and the list of the published articles.

Selected references

[1] R. Gheorghe, M. Andruh, A. Muller, M. Schmidtmann, *Inorg. Chem.*, **41**, 5314 (2005); R. Gheorghe, P. Cucoş, M. Andruh, J. –P. Costes, B. Donnadieu, S. Shova, *Chem. Eur. J.*, **12**, 187 (2006).

[2] M. Andruh, *Chem. Commun.*, 2565 (2007); M. Andruh, *Chem. Commun.*, **47**, 3025 (2011).

[3] P. Forlano, L.M. Baraldo, J. A. Olabe, C. O. Dellavedova, *Inorg. Chim. Acta*, **223**, 37 (1994); L. A. Genti, A. Navaza, J. A. Olabe, G. E. Rigotii, *Inorg. Chim. Acta*, **179**, 89 (1994); P. Albores, L. D. Slep, L. M. Baraldo, R. Baggio, M. T. Garland, E. Rentschler, Inorg. Chem., **45**, 2361 (2006); A. Chilesotii, *Gazz. Chim. Ital.*, **34II**, 493 (1904); (b) O. Olsson, *Z. Anorg. Allg. Chem.*, **88**, 49 (1914); J. G. Leipold, L. D. C. Bok, P. J. Cillier, *Z. Anorg. Allg. Chem.*, **409**, 343 (1974).

[4] A. Dogaru, C. Pichon, R. Ababei, D. Mitcov, C. Maxim, L. Toupec, C. Mathonière, R. Clérac, M. Andruh, *Polyhedron*, **75**, 146 (2014).